DOI: 10.1002/smll.200600067

Formation of CdS Nanoparticle Necklaces with Functionalized Dendronized Polymers

Yanhong Zhang, Yongming Chen, Haijun Niu, and Mingyuan Gao**

A one-dimensional assembly of cadmium sulfide (CdS) nanoparticles was prepared by using functionalized polymers with pendant Fréchet-type dendritic wedges of different generation. The novel dendronized polymers acted as both nanoreactors for the formation of CdS nanoparticles and a template to arrange the nanoparticles into a necklace. The polymers of different dendron generation were applied to stabilize CdS particles and the effect of dendron size was observed. CdS nanoparticle necklaces were obtained successfully when polymers bearing second-generation dendrons were applied.

Keywords:
- cadmium sulfide
- dendronized polymers
- nanoparticles
- semiconductors
- templates

1. Introduction

The syntheses of inorganic semiconductor nanoparticles have motivated much interest due to their size-dependent optical and electronic properties, and potential applications in the fields of nonlinear optics, light-emitting devices, electronics, and so on. Control of the particle size and polydispersity is very important due to the quantum confinement effect.[1] Many materials, such as polymers, ceramics, and glasses, have been used as the matrix to disperse the semiconductor nanocrystals.[2] Cadmium sulfide (CdS) nanoparticles have been prepared by using organic polymers of styrene-based random ionomers,[3] diblock ionomers,[4] double-hydrophilic block copolymers,[5] or polymer micelles.[6–9] In these cases the polymers act as stabilizers or nanoreactors for the formation of semiconductor nanoparticles. Dendrimers can also play this role, and semiconductor or metal nanoparticles have been synthesized in poly(amidoamine) (PAMAM) or other dendrimers.[10–15] Furthermore, linear templates, such as polyelectrolytes,[16] DNA,[17] proteins,[18] and carbon nanotubes,[19] or template-free self-assembly methods,[20] have been applied to prepare one-dimensional (1D) assemblies of nanoparticles. When these narrowly dispersed nanoparticles are arranged along the polymer chains, semiconductor or metal nanowires may be formed and many collective properties that are evidently different from single nanoparticles can be expected for the 1D nanoparticle assemblies.[21] However, organization of these nanoparticles into a linear form is still difficult. Gold nanowires and wirelike cadmium sulfide nanoparticle assemblies using core–shell cylindrical polymer brushes as templates have been synthesized successfully.[22,23] In these cases, the cylindrical polymers act not only as nanoreactors and stabilizers for the formation of nanoparticles, but also as templates to induce the arrangement of the nanoparticles. However, examples of the assembly of inorganic nanoparticles in one dimension with rationally designed single molecules are rather scarce. Well-defined synthetic polymers with tunable conformation may be more suitable for such purposes, compared with naturally occurring polymer products.

Dendronized polymers, which emerged in the early 1990s, are hybrids of dendritic wedges and linear polymers.[24,25] The pendant dendrons tune polymer-chain morphology, and therefore the polymer properties, through steric hindrance. With increasing growth of the dendrons, the steric repulsion between the dendritic wedges along the

---

[*] Dr. Y. Zhang, Prof. Y. Chen
State Key Laboratory of Polymer Physics and Chemistry
Joint Laboratory of Polymer Sciences and Materials
Institute of Chemistry, The Chinese Academy of Sciences
Beijing 100080 (China)
Dr. Y. Zhang, Prof. Y. Chen, H. Niu, Prof. M. Gao
Key Laboratory of Colloid, Interface Science and
Chemical Thermodynamics
Institute of Chemistry, The Chinese Academy of Sciences
Beijing 100080 (China)
Fax: (+86) 10-62559373
E-mail: ymchen@iccas.ac.cn
gaomy@iccas.ac.cn

backbone increases, and as a result, the main polymer chains extend and transform from random coils to rodlike cylinders. Much attention has been paid to their synthesis;[26] however, their potential applications have been scarcely studied despite the expectation that such polymers can be applied in nanotechnology.[27]

If functional groups are introduced along the dendronized polymer backbones they become buried within the molecular cylinders provided the dendritic wedges are large enough.[28] Therefore, incorporation of functional groups along the main chains of dendronized polymers is very important for exploring the applications of one-dimensional nanoarrays wrapped by dendron wedges. Dendronized cyclo-copolymers bearing pyrrolidinopyridine functional groups along the backbone have been reported and used as a catalyst for an esterification reaction.[29] Recently, we reported reactive dendronized copolymers of maleic anhydride (MA) and styryl macromonomers, which carry Fréchet-type polyether dendrons of the first to the fourth generation.[30] Owing to the activity of the anhydride, such dendronized polymers can act as a molecular scaffold for studying 1D nanomaterials. Hydrolysis and amidolysis reactions have been applied to these dendronized copolymers, and a series of copolymers with dendron-*alt*-2(COOH) and dendron-*alt*-linear alkyl chain structures were obtained.

Herein, we report the formation of inorganic-nanoparticle necklaces by using pyridine-functionalized dendronized polymers bearing Fréchet-type polyether dendrons. The functionalized copolymers (G*n*MA-*g*-AP) were synthesized via the reaction of reactive dendronized copolymers (G*n*MA) with 2-aminopyridine (AP) (Scheme 1); as a result, pyridine and carboxyl groups are introduced by amidolysis along the backbones of the dendronized polymers. Compared to other molecular templates, the cross section of the dendronized polymer can be controlled precisely since the pendant dendron wedges are prepared by stepwise organic reactions. With an increase of the pendant dendron generation, and therefore, greater steric repulsion between the bulky side groups, the flexibility of the dendronized polymers can be changed. The functional groups may coordinate with Cd^{2+} ions and fix the spatial site of nucleation along the main chain.

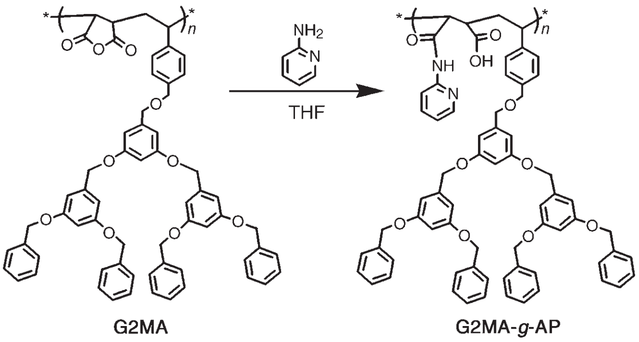

Scheme 1. Amidolysis of a second-generation dendronized copolymer. THF: tetrahydrofuran.

2. Results and Discussion

2.1. Synthesis of Dendronized Copolymers G*n*MA-*g*-AP ($n = 1$–4)

The molecular weights and polydispersity indexes of the precursor dendronized copolymers G*n*MA ($n = 1$–4) used in this experiment for preparation of G*n*MA-*g*-AP are listed in Table 1. Long polymer chains were required to form the 1D nanoparticle array. As indicated in Table 1, the reactive dendronized polymer precursors G*n*MA ($n = 1$, 2) had a very high degree of polymerization (DP), which was confirmed from static light-scattering measurements. For example, the DP for G1MA and G2MA used in this article was 790 and 580, respectively; one repeat unit (defined as the combination of one dendritic monomer and one succinic anhydride unit) contributed to four C–C bonds along the polymer backbone. The DP for G3MA and G4MA was relatively low due to the steric hindrance of the higher-generation dendritic wedges to the copolymerization. The amidolysis reactions of the dendronized copolymer G*n*MA ($n = 1$–4) with primary amines have been described in detail previously,[30] and the reactions can be confirmed by Fourier transform infrared (FTIR) spectra (see Experimental Section). After reaction with 2-aminopyridine (AP), the characteristic absorbance of anhydride at 1861 cm^{-1} and 1779 cm^{-1} disappeared in the FTIR spectra, while that of amide at 1715 cm^{-1} became apparent. Furthermore, elemental analysis has shown that the molar ratio of AP and the repeat unit (RU) is 0.8:1, 0.9:1, 0.9:1, and 1.1:1 for G1MA-*g*-AP to G4MA-*g*-AP, respectively. Also, ^1H NMR spectroscopic analysis has been used to characterize these products. Though the chemical shift of the proton resonances did not change markedly, the integrated area over the range of 7.5–6.0 ppm increased, which can be attributed to the introduction of pyridine groups. Therefore, the functionalization ratios are rather high and AP has been grafted to the dendronized polymer backbones as expected. In addition, the amidolysis concurrently produced COOH groups.

Table 1. Properties of the dendronized copolymers G*n*MA ($n = 1$–4).

Sample	M_w/M_n[a]	M_w[b]	M_w RU[c]	DP_w[d]
G1MA	1.34	424000	534.6	790
G2MA	1.26	558900	959.1	580
G3MA	2.62	349900	1808.1	190
G4MA	1.37	309000	3506.0	88

[a] Results obtained by using size-exclusion chromatography. [b] As calculated from static light-scattering (SLS) experiments. [c] Molecular weight of the repeat unit (which consists of one pair of dendritic monomers and one succinic anhydride). [d] Degree of polymerization calculated from the M_w values determined by SLS measurements.

2.2. Formation of CdS Nanoparticles

The preparation of CdS nanoparticles involved two steps: First, Cd^{2+} ions were coordinated with pyridine and carboxylic acid groups located along the polymer backbones. Second, H_2S gas was introduced and CdS nanocrystals were produced in situ. The coordination of Cd^{2+} ions and carboxylic acid between the polymer of G1MA-*g*-AP and cadmium acetate was confirmed by FTIR spectroscopy as indicated in Figure 1. After complexation, the band at 1779 cm^{-1} corresponding to an asymmetric vibration of the carbonyl group in the polymer shifted to 1558 cm^{-1}.[31] However, the weak shift from 1590 to 1600–1620 cm^{-1} corresponding to the complexation of pyridine and metal ions[7] cannot be discerned due to the broad and strong absorbance of benzene rings at 1595 cm^{-1}.

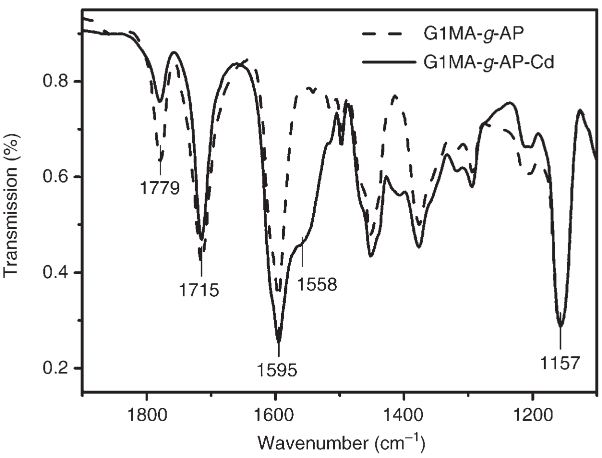

Figure 1. FTIR spectra of the polymer G1MA-*g*-AP and its complex with cadmium acetate. The spectra have been normalized at 1157 cm^{-1}.

The influence of the molar ratio of cadmium ions to the RU of the dendronized polymer on the CdS nanoparticles was explored by using the dendronized copolymer bearing the second-generation dendrons (G2MA-*g*-AP). The concentration of G2MA-*g*-AP in THF was maintained at 2.5 $mg\,mL^{-1}$, while the molar ratio of Cd:RU was varied between 0.5:1, 1:1, and 2:1, and H_2S was bubbled through the solution for 10 min. When H_2S was introduced, the solution changed from colorless to light yellow immediately, implying the formation of CdS nanoparticles. A typical transmission electron microscopy (TEM) image of the nanoparticles is shown in Figure 2 (the inset shows the associated electron diffraction pattern). It was interesting to note that the nanoparticles were aligned in a "necklace" pattern; individual particles were never observed. The particle size (estimated from the TEM image) was in the range of 3–4 nm. The *d* spacings calculated from the rings in the electron diffraction patterns were 0.36, 0.22, and 0.19 nm, corresponding to the (111), (220), and (311) lattice planes of the cubic phase of CdS. No matter which feed ratio was used, this kind of necklace morphology was always formed. Therefore, as expected, the CdS nanoparticles were arranged into 1D assemblies with the aid of the dendronized polymers.

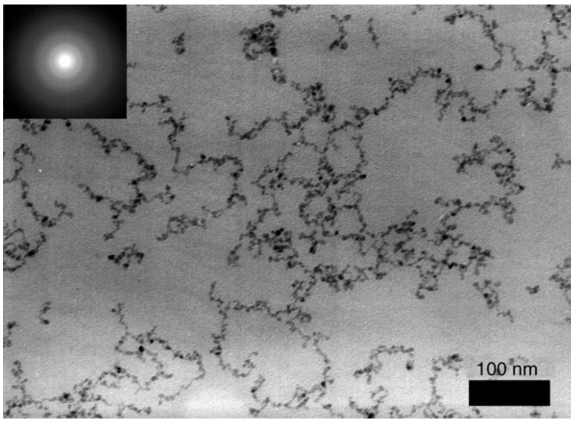

Figure 2. TEM image of CdS nanoparticle necklaces formed with the aid of polymer G2MA-*g*-AP. The molar ratio of Cd:RU was 1:1 and the polymer concentration in THF was 2.5 $mg\,mL^{-1}$.

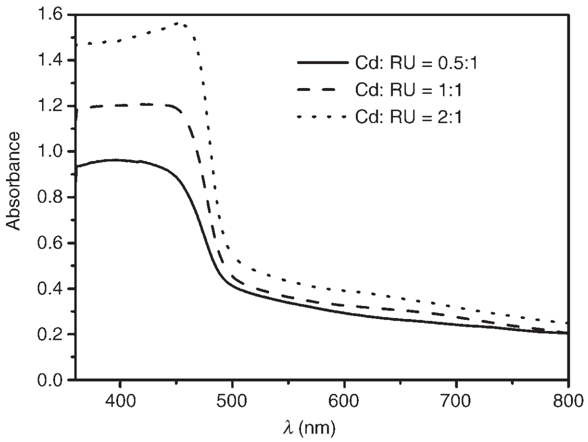

Figure 3. UV/Vis spectra of CdS nanoparticles formed in the polymer G2MA-*g*-AP with different molar ratios of Cd:RU. The concentration of G2MA-*g*-AP in THF was 2.5 $mg\,mL^{-1}$.

To further characterize the CdS nanoparticles, UV/Vis absorption spectra were collected, as shown in Figure 3. Similar curves were obtained even when the feed ratios were changed. The absorption edge (λ_e) was obtained from the intersection of the sharply decreasing region of the spectrum with the baseline as a reference.[3] The exciton maximum (λ_m) is the wavelength where absorption is at its highest. CdS particle sizes were calculated from the λ_e and λ_m values according to Henglein's empirical curve.[1] On increasing the ratio of Cd:RU from 0.5:1 to 2:1, the value of λ_e decreased from 499 to 494 nm, while that of λ_m increased from 415 to 452 nm. These results yield a sharper absorption curve (as shown in Figure 3), indicating that the size distribution of the CdS particles became narrower. The absorption edge was blue-shifted relative to the absorption onset of bulk CdS (515 nm), thus showing a quantum confinement effect. But the particles produced from three Cd:RU ratios did not differ greatly, which agreed with the TEM results. It was noteworthy that scattering was observed in the absorption curves despite the fact that the CdS particle size was quite small. Considering the very high molecular weight of the template polymer, it is believed that the scattering was due to the size of whole CdS/polymer necklace hybrids, rather than individual nanoparticles.

The formation of CdS particle necklaces using different polymer concentrations was also studied. The concentration of the polymer G2MA-*g*-AP in THF was switched between 1.0, 2.5, and 5.0 mg mL^{-1} while the molar ratio of Cd:RU was kept at 1:1; H_2S gas was bubbled through the solution for ten minutes. The results given from TEM and absorption spectra indicated that the polymer concentration had little influence on particle size when other conditions were kept the same. The shape of the CdS necklaces formed in these experiments were very similar to those described above.

Dendronized polymers of different generation were also applied to induce the formation of CdS nanoparticles. Figure 4 shows a TEM image of CdS particles formed in the presence of G1MA-*g*-AP. In contrast to the results from G2MA-*g*-AP, the CdS nanoparticles formed wide strips although the individual particle sizes calculated from values of λ_e and λ_m were still small. Therefore, the dendronized copolymer with smaller dendritic wedges did not efficiently stabilize the necklaces. When dendronized copolymers of higher generation (G3MA-*g*-AP and G4MA-*g*-AP) were applied, some light-yellow precipitates were observed in solution after H_2S gas was introduced, revealing that these polymers failed to stabilize the CdS crystals. The clear solutions were taken for TEM analysis and, instead of CdS nanoparticle necklaces, only small, randomly dispersed nanoparticles were found. Therefore, most of CdS had been precipitated. This result is very different to the case with lower-generation dendritic wedges, which is unexpected.

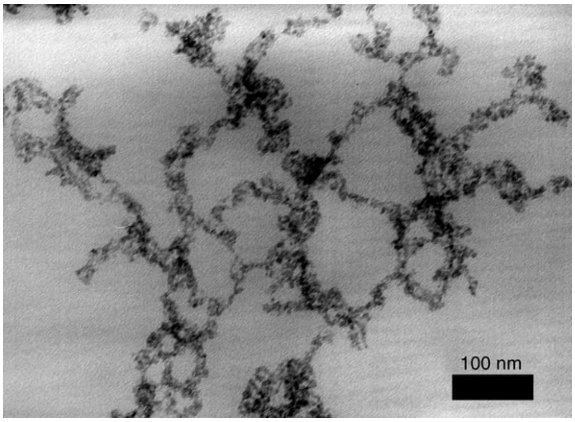

Figure 4. TEM image of CdS nanoparticles formed in polymer G1MA-*g*-AP. The polymer concentration was 2.5 mg mL^{-1} and the molar ratio of Cd:RU was 1:1.

The results described above have demonstrated that CdS nanoparticle necklaces were prepared successfully with the aid of the functionalized dendronized copolymers, in which the size of the dendritic wedges had a significant influence; a suitable dendron size is important for the arrangement of the CdS nanoparticles. In this work, G2MA-*g*-AP, which bears second-generation dendrons, may organize CdS nanoparticles into 1D arrays. Larger pendant dendrons or smaller dendrons are not able to induce the necklace formation. For the smallest dendronized polymer, G1MA-*g*-AP, the dendron is too small and the polymer chain is too flexible to organize the CdS particles. Furthermore, the small dendron wedges could not prevent the CdS nanoparticles from agglomerating. These factors are not helpful for forming well-defined single necklaces. Scheme 2a provides a schematic representation of a possible mechanism for the formation of CdS nanoparticles with G1MA-*g*-AP.

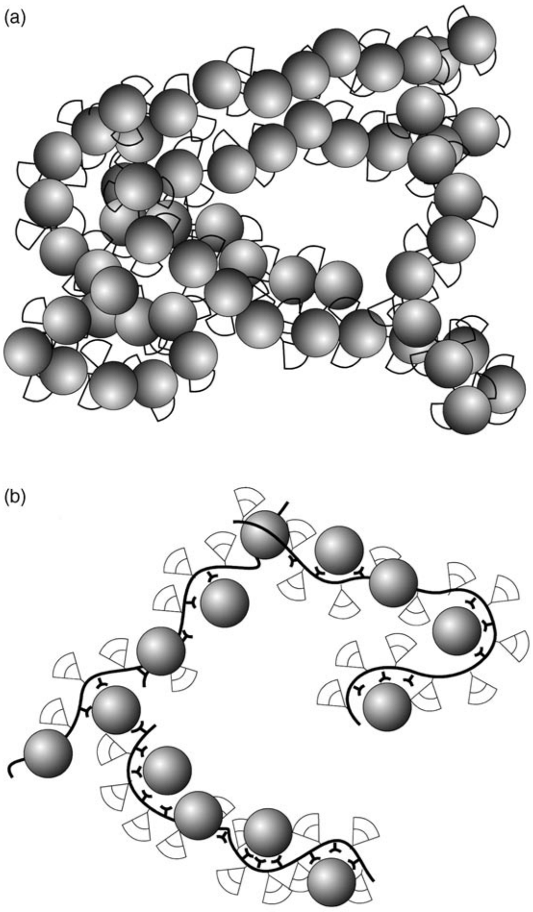

Scheme 2. Schematic showing the appearance of CdS nanoparticles formed in polymers G1MA-*g*-AP (a) and G2MA-*g*-AP (b).

In contrast, second-generation dendritic wedges may endue the polymer chain with enhanced rigidity, although it is far from a compact packing. There is space between two adjacent dendrons, in which the nanocrystals can be accommodated. However, the size of the CdS particles, as given by TEM, was ≈3 nm, and it appears that second-generation dendrons cannot shield the nanoparticles from aggregation. In addition, one pyridine and one COOH group are apparently not enough to bind one particle. Thus, intra- or intermacromolecular multivalent binding is necessary to capture particles. In order to clarify this mechanism, atomic force microscopy (AFM) analysis of the necklaces was carried out. In Figure 5, similar necklaces were observed as those shown in the TEM images. The size of the "bubbles" in the image is ≈7–11 nm, which represents CdS particles encapsulated by the dendrons. The diameter of the line between the bubbles is ≈3 nm, which is in agreement with the size of a single dendronized polymer chain[32] after considering the

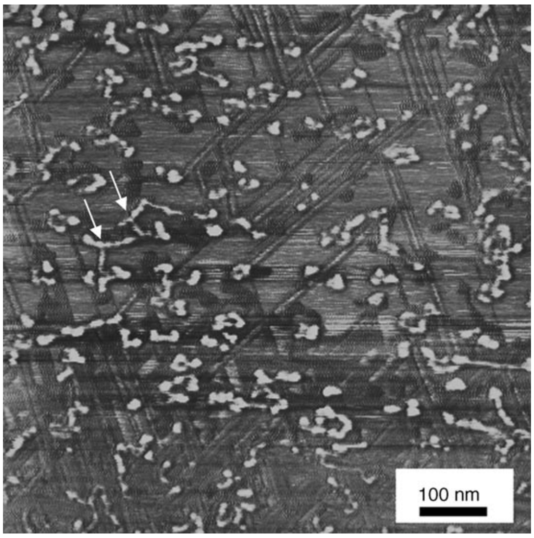

Figure 5. AFM phase image of CdS nanoparticles on polymer G2MA-*g*-AP, spin-coated from a THF solution onto highly oriented pyrolytic graphite (HOPG). (vertical scale: 20°; the arrows indicate a branched site.)

error due to tip resolution. Therefore, one CdS particle can be stabilized by the loop of one polymer segment via multivalent interaction. It is noteworthy that some branched necklaces were found as indicated by the arrows in Figure 5, disclosing that a stabilizing interaction from different polymers is also possible.

Based on these results, the formation of CdS nanoparticle necklaces is presented schematically in Scheme 2b. The particles were mainly stabilized by intramolecular multivalent interactions through folding of the dendronized polymer. Unlike the CdS nanoparticles formed with the polymer G1MA-*g*-AP, the greater dendron size of the polymer G2MA-*g*-AP is needed to prevent more molecular chains from agglomeration. With the increase in dendritic wedge size, the copolymer becomes more rigid and bending the chain to stabilize the particles by multivalent interactions becomes more difficult. A single pair of pyridine and COOH groups is not strong enough and, therefore, the formed CdS particles are prone to precipitate. This could be the reason that the G3MA-*g*-AP and G4MA-*g*-AP failed to aid the formation of nanonecklaces.

3. Conclusions

Through an amidolysis reaction, pyridine-functionalized copolymers bearing a different generation of Fréchet-type dendritic wedges were prepared. These well-defined dendronized copolymers were applied as stabilizers and templates for the formation of CdS nanoparticle necklaces. Cadmium ions were coordinated with the pyridine and carboxyl groups along the main chain of the polymer, and CdS nanoparticles were synthesized by reaction with H_2S. The dendron size had a strong impact on necklace formation. With second-generation polymers, CdS nanoparticle necklaces were prepared successfully. However, polymers of the first, third, and fourth generation failed to produce such necklaces, which could be explained by a combination of dendron size and chain flexibility. These results demonstrate that only suitable functionalized dendronized polymers are needed to organize the CdS nanoparticles into 1D arrays. This finding reveals that functionalized dendronized polymers may be applied as single-molecular scaffolds to organize inorganic nanoparticles.

4. Experimental Section

Materials: 2-Aminopyridine (99%, Merck) and cadmium acetate dihydrate ($Cd(OAc)_2\cdot 2H_2O$; 99.5%, the Second Factory of Tianjin Chemicals Co.) were used as received. H_2S gas was produced by dropping the aqueous solution of sodium sulfide (Na_2S) to concentrated hydrogen chloride aqueous (36–38%). The dendronized alternating copolymers G*n*MA were synthesized as described previously;[30] G*n* stands for dendron of generation *n* and MA stands for maleic anhydride unit. The properties of the dendronized copolymer G*n*MA for preparation of G*n*MA-*g*-AP in this article are listed in Table 1.

Characterization: FTIR spectra were recorded by a deuterate triglycine sulfate (DTGS) detector on Bruker EQUINOX 55 spectrometer and processed by the Bruker OPUS program. The samples were twice precipitated in diethyl ether and once in hexane and dried in a vacuum desiccator in order to remove the influence of the uncoordinated cadmium acetate in solution. The white powder obtained in this way was dissolved in THF; the solution (20 $mg\,mL^{-1}$) was then dropped on a KBr flake and dried before tested.

UV/Vis absorption spectra were recorded on a Shimadzu UV/Vis spectrophotometer (UV-1601PC) by scanning the CdS-containing solution in a 1-cm quartz cell. The scanning range was from 200 to 800 nm. Absorption from the solvent was subtracted from each spectrum automatically.

TEM measurements were performed on a Zeiss EM 10 A transmission electron microscope operated at 100 kV. TEM samples were prepared by depositing a droplet of CdS-containing solution onto a TEM grid which had been coated with carbon film. The particle size was the average of 20 particles in a TEM image and the particle-size distribution was narrow.

AFM images were obtained under ambient conditions using a Digital Instrument Multimode Nanoscope IIIA operating in the tapping mode. Si cantilever tips (TESP) with a resonance frequency of approximately 300 kHz and a spring constant of about 40 $N\,m^{-1}$ were used. The scan rate varied from 0.5 to 1.5 Hz. The set-point amplitude ratio was maintained at 0.9 to minimize the sample deformation induced by the tip. All AFM images were subjected to a first-order plane fitting procedure to compensate for sample tilt. The samples for tapping-mode AFM measurements were prepared by spin-casting on HOPG at 2000 rpm of dilute solutions.

General procedure for the amidolysis of the copolymer GnMA (n = 1–4) and synthesis of GnMA-g-AP (n = 1–4): The copolymer G*n*MA ($n = 1$–4) and AP were mixed in an ampoule at a molar ratio of 1:1.1 (for $n = 1$, 3, 4) or 1:2.5 (for $n = 2$), and THF was added to make the concentration of G*n*MA ($n = 1$–4) 50 mg mL^{-1}. The ampoule was sealed and kept in an oil bath at 70 °C for 48 h. After removal of most of the solvent, the reaction mixture was twice precipitated from diethyl ether and once from hexane. The product was dried in a vacuum desiccator overnight, and collected as a white powder (yield > 90 %). The reaction was confirmed by FTIR spectroscopy (Figure 6). After reaction, the characteristic peaks of anhydride at 1861 and 1779 cm^{-1} have disappeared except for G1MA-g-AP. Elemental analyses: G1MA-*g*-AP: Calcd for $(C_{39}H_{36}N_2O_6)_n$: N 4.46, C 74.51, H 5.77 %; found: N 3.00, C 73.58, H 5.80 %. G2MA-*g*-AP: Calcd for $(C_{67}H_{60}N_2O_{10})_n$: N 2.66, C 76.41, H 5.74 %; found: N 2.05, C 74.57, H 5.81 %. G3MA-*g*-AP: Calcd for $(C_{123}H_{108}N_2O_{18})_n$: N 1.47, C 77.67, H 5.84 %; found: N 1.17, C 76.24, H 5.84 %. G4MA-*g*-AP: Calcd for $(C_{235}H_{204}N_2O_{34})_n$: N 0.78, C 78.40, H, 5.71 %; found: N 1.00, C 76.94, H 5.82 %. The molar ratios of AP:RU deduced from the nitrogen content in the elemental analyses were 0.8:1, 0.9:1, 0.9:1, and 1.1:1 for G1MA-*g*-AP to G4MA-*g*-AP, respectively.

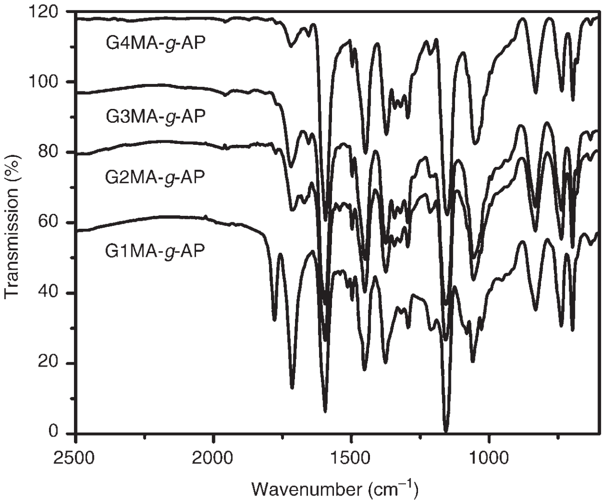

Figure 6. FTIR spectra of G*n*MA-*g*-AP ($n = 1$–4).

Preparation of CdS nanoparticles: The polymers G*n*MA-*g*-AP ($n = 1$–4) were dissolved in THF (2 mL) to a desired concentration. After stirring for 1 h, $Cd(OAc)_2 \cdot 2H_2O$ (0.05 mmol mL^{-1}), in a calculated volume of THF and CH_3OH (2:1 v/v), was added. At this time, the solution appeared colorless and transparent. After stirring for another 24 h, H_2S gas was bubbled through for 10 min and the color of the solution turned yellow.

Acknowledgements

Financial support from the Chinese Academy of Sciences and Chinese NSF (20534010) is gratefully acknowledged.

---

[1] A. Henglein, *Chem. Rev.* **1989**, *89*, 1861 – 1873.
[2] L. L. Beecroft, C. K. Ober, *Chem. Mater.* **1997**, *9*, 1302 – 1317.
[3] a) M. Moffitt, A. Eisenberg, *Chem. Mater.* **1995**, *7*, 1178 – 1184; b) Q. Dai, J. G. Worden, J. Trullinger, Q. Huo, *J. Am. Chem. Soc.* **2005**, *127*, 8008 – 8009.
[4] M. Moffitt, L. McMahon, V. Pessel, A. Eisenberg, *Chem. Mater.* **1995**, *7*, 1185 – 1192.
[5] L. M. Qi, H. Cölfen, M. Antonietti, *Nano Lett.* **2001**, *1*, 61 – 65.
[6] M. Moffitt, H. Vali, A. Eisenberg, *Chem. Mater.* **1998**, *10*, 1021 – 1028.
[7] H. Y. Zhao, E. P. Douglas, B. S. Harrison, K. S. Schanze, *Langmuir* **2001**, *17*, 8428 – 8433.
[8] H. Y. Zhao, E. P. Douglas, *Chem. Mater.* **2002**, *14*, 1418 – 1423.
[9] J. G. Zhang, S. Q. Xu, E. Kumacheva, *J. Am. Chem. Soc.* **2004**, *126*, 7908 – 7914.
[10] B. K. Sooklal, L. H. Hanus, H. J. Ploehn, C. J. Murphy, *Adv. Mater.* **1998**, *10*, 1083 – 1087.
[11] R. W. J. Scott, A. K. Datye, R. M. Crooks, *J. Am. Chem. Soc.* **2003**, *125*, 3708 – 3709.
[12] Y. A. Wang, J. J. Li, H. Y. Chen, X. G. Peng, *J. Am. Chem. Soc.* **2002**, *124*, 2293 – 2298.
[13] W. H. Guo, J. J. Li, Y. A. Wang, X. G. Peng, *J. Am. Chem. Soc.* **2003**, *125*, 3901 – 3909.
[14] B. I. Lemon, R. M. Crooks, *J. Am. Chem. Soc.* **2000**, *122*, 12 886 – 12 887.
[15] H. F. Lang, R. A. May, B. L. Iversen, B. D. Chandler, *J. Am. Chem. Soc.* **2003**, *125*, 14 832 – 14 836.
[16] S. Minko, A. Kiriy, G. Gorodyska, M. Stamm, *J. Am. Chem. Soc.* **2002**, *124*, 10 192 – 10 197.
[17] T. Torimoto, M. Yamashita, S. Kuwabata, T. Sakata, H. Mori, H. Yoneyama, *J. Phys. Chem. B* **1999**, *103*, 8799 – 8803.
[18] X. Fu, Y. Wang, L. Huang, Y. Sha, L. Gui, L. Lai, Y. Tang, *Adv. Mater.* **2003**, *15*, 902 – 906.
[19] M. J. Moghaddam, S. Taylor, M. Gao, S. Huang, L. Dai, M. J. McCall, *Nano Lett.* **2004**, *4*, 89 – 93.
[20] Z. Y. Tang, B. Ozturk, Y. Wang, N. A. Kotov, *J. Phys. Chem. B* **2004**, *108*, 6927 – 6931.
[21] Z. Y. Tang, N. A. Kotov, *Adv. Mater.* **2005**, *17*, 951 – 962.
[22] R. Djalali, S. Y. Li, M. Schmidt, *Macromolecules* **2002**, *35*, 4282 – 4288.
[23] M. F. Zhang, M. Drechsler, A. H. E. Müller, *Chem. Mater.* **2004**, *16*, 537 – 543.
[24] H. Frauenrath, *Prog. Polym. Sci.* **2005**, *30*, 325 – 384.
[25] a) D. A. Tomalia, A. M. Naylor, W. A. Goddard III, *Angew. Chem.* **1990**, *102*, 119 – 157; *Angew. Chem. Int. Ed.* **1990**, *29*, 138 – 175; b) V. Percec, J. Heck, *J. Chem. Soc. Perkin Trans. 1* **1993**, 2799 – 2811; c) C. J. Hawker, J. M. J. Frechét, *Polymer* **1992**, *33*, 1507 – 1511; d) R. Freudenberger, W. Claussen, A. D. Schlüter, H. Wallmeier, *Polymer* **1994**, *35*, 4496 – 4501.
[26] A. F. Zhang, L. J. Shu, Z. S. Bo, A. D. Schlüter, *Macromol. Chem. Phys.* **2003**, *204*, 328 – 339.
[27] A. D. Schlüter, J. P. Rabe, *Angew. Chem.* **2000**, *112*, 860 – 880; *Angew. Chem. Int. Ed.* **2000**, *39*, 864 – 883.
[28] H. Frey, *Angew. Chem.* **1998**, *110*, 2313 – 2318; *Angew. Chem. Int. Ed.* **1998**, *37*, 2193 – 2197.
[29] C. O. Liang, B. Helms, C. J. Hawker, J. M. J. Fréchet, *Chem. Commun.* **2003**, 2524 – 2525.
[30] Y. H. Zhang, J. Huang, Y. M. Chen, *Macromolecules* **2005**, *38*, 5069 – 5077.
[31] L. D. Sun, X. F. Fu, M. W. Wang, C. H. Liu, C. S. Liao, C. H. Yan, *J. Lumin.* **2000**, *87*, 538 – 541.
[32] W. Stocker, B. L. Schürmann, J. P. Rabe, S. Förster, P. Lindner, I. Neubert, A. D. Schlüter, *Adv. Mater.* **1998**, *10*, 793 – 797.

Received: February 7, 2006
Revised: May 5, 2006